

# Ceramic-metal reaction welding

H. J. DE BRUIN

*The Flinders University of South Australia, Bedford Park, South Australia, 5042*

A. F. MOODIE, C. E. WARBLE

*Division of Chemical Physics, CSIRO, P.O. Box 160, Clayton, Victoria, Australia 3168*

In bonding ceramic oxides to metals, two reaction mechanisms have been utilized. These are (1) a surface or microscopic reaction, between close-packed ceramic oxides, quartz, and glasses and the noble metals (e.g. Pt, Pd, Au, Ag), maintaining a sharp discontinuity at the interface, (2) a bulk or macroscopic reaction between the same oxides and other transition metals (e.g. Fe, Co, Ni) producing a diffusional type interface. Both have common reaction conditions and occur: (a) below the melting point of the lowest melting component, (b) in any atmosphere compatible with all components at the operating temperature, (c) under little or no pressure, and (d) without deformation.

The progress of several Type 1 reactions has been followed by direct observation at elevated temperatures and high resolution in a modified transmission electron microscope. It has thereby been established that this reaction proceeds with the formation of an intermediate phase, liquid-like at temperatures below the melting point of any of the components.

Bonds have also been examined using electron scanning microscopy, electron probe microanalysis, and optical microscopy. Vacuum tight bonds can be produced and shear tests indicate that strength is generally limited by the strength of oxide components.

## 1. Introduction

Conventional techniques for bonding ceramics to metals and other ceramics are based largely on the brazing principle, in which an intermediate liquid filler – either metal or glass – wets the surfaces to be joined. Few metals will wet oxide ceramics other than Ti and Ti-based alloys. Alternatively sophisticated procedures have been developed to “metallize” the oxide surface prior to electroplating and conventional brazing [1, 2].

Several patents describe techniques for directly bonding ceramics to metals in the solid state under a variety of conditions [3-7], Klomp [8, 9] in particular having carried out work on bonds involving alumina. Indeed in one guise or another [10, 11] this type of bonding has probably been encountered by many workers, but no explanation of the mechanisms, consistent with all of the experimental evidence has been given. The outline of a mechanism specific to their materials, and which accounts for most of their observations, has been given by Calow, Bayer and

Porter [12, 13] who have recently investigated the bonding of Ni, Cr, and nichrome to  $Al_2O_3$ . An observation by Moodie and Warble [14, 15] in the transmission electron microscope strongly suggests the existence of a hitherto unknown surface reaction between oxide ceramics and metals that could form the basis of a plausible explanation for at least our Type 1 reaction.

It is the purpose of this communication to describe two types of ceramic-metal reactions that lead to the formation of very strong bonds, and to present new experimental evidence which limits the possible mechanisms.

Table I shows a list of systems which undergo one or other of the two types of reactions: Type 1 involving the noble metals and Type 2 the remaining metals in the transition series. Both reactions lead to the formation of strong bonds with a wide range of oxides including silicates. Preliminary accounts of some of the practical aspects of these interactions have been reported [16-18] and patent applications have been filed in Australia [19] and several other countries.

TABLE I Representative bonds

Type 1 reaction	Type 2 reaction
MgO/Pt/MgO	MgO/Ni/MgO
MgO/Pd/MgO	Al <sub>2</sub> O <sub>3</sub> /Ni/Al <sub>2</sub> O <sub>3</sub>
Al <sub>2</sub> O <sub>3</sub> /Pt/Al <sub>2</sub> O <sub>3</sub>	Al <sub>2</sub> O <sub>3</sub> /Ti/Al <sub>2</sub> O <sub>3</sub>
Al <sub>2</sub> O <sub>3</sub> /Pd/Al <sub>2</sub> O <sub>3</sub>	BeO/Ni/BeO
Al <sub>2</sub> O <sub>3</sub> /Au/Al <sub>2</sub> O <sub>3</sub>	BeO/Fe/MgO
BeO/Pt/Graphite	Brick/Ni/Brick
Ferrite/Pt/Ferrite	SiO <sub>2</sub> /Cu/SiO <sub>2</sub>
ZrO <sub>2</sub> */Pt/ZrO <sub>2</sub> *	Cu/BeO/Cu
UO <sub>2</sub> /Pt/BeO	
SiO <sub>2</sub> /Pt/SiO <sub>2</sub>	
SiO <sub>2</sub> /Au/Glass	
SiO <sub>2</sub> /Au/SiO <sub>2</sub>	
SiO <sub>2</sub> /Ag/SiO <sub>2</sub>	
Glass/Au/Glass	

\*Scandia stabilized.

Whether the oxide is single crystal or polycrystalline and, in particular, whether SiO<sub>2</sub> is in the form of quartz, optical quality fused silica, or opaque fused silica makes only detailed differences in bond formation.

## 2. Experimental procedures

### 2.1. Method for making ceramic/metal/ceramic couples

Oxide cylinders, 0.5 in. diameter and 0.25 in. high were cold-pressed (20 tsi) and sintered at 1500°C in dry nitrogen for 6 h (Al<sub>2</sub>O<sub>3</sub> and MgO) or at 1750°C in hydrogen for 60 h (BeO). These high density polycrystalline compacts are specified in Table II. The metal foils used were cold rolled and annealed, and are specified in Table III.

The specimens were held between boron nitride supports in the centre of a nichrome or platinum wound tube furnace. A slight pressure (about 100 kNm<sup>-2</sup>) was applied by releasing an air-cooled spring on top of the rig and the temperature controlled with a Eurotherm proportional regulator to within 2°C of the required operating temperature.

### 2.2. Methods for testing and examining bonds

Relative shear strengths were determined because

TABLE III Specification of metal foils

Metal	Thickness inch	Purity %	Major impurities in order of significance
Au	0.002	99.3 +	Cu, Ag, and As
Pd	0.0005	99.5	Ni, Pt
Pt	0.001	99.9 +	Pd, Ni
Ni	0.004	99.3	Fe, Co

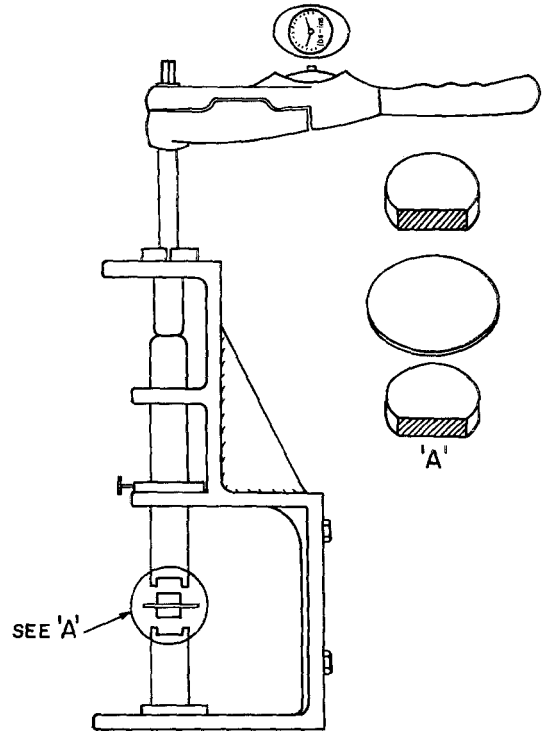


Figure 1 Assembly designed for measuring relative shear strengths of the couples.

dimensional restrictions made tensile tests impracticable. The oxide cylinders were ground prior to assembly with a flat edge fitting precisely into the testing device (Fig. 1). An applied torque was measured until failure of the couple occurred. Other couples were then cut at right angles to the metal layer and polished. Optical micrographs were taken on a Reichert Zetopan microscope.

TABLE II Specification of ceramic oxide specimens

Material	Origin	Relative density %	Impurity content (ppm)	Average grain size $\mu\text{m}$
Al <sub>2</sub> O <sub>3</sub>	Linde "A"	97.1	Mg(10), Cu(100), Fe(500), Si(100)	55
MgO	Merck's AR MgCO <sub>3</sub> calcined at 900° for 1 h	95.0	Fe(20), Zn(50), Al(50), Ba(10), Cu(500), Pb(10)	45
BeO	UOX	96.8	Al(15), Fe(200), Mg(9), Pb(20), Si(250), Ba(5)	60

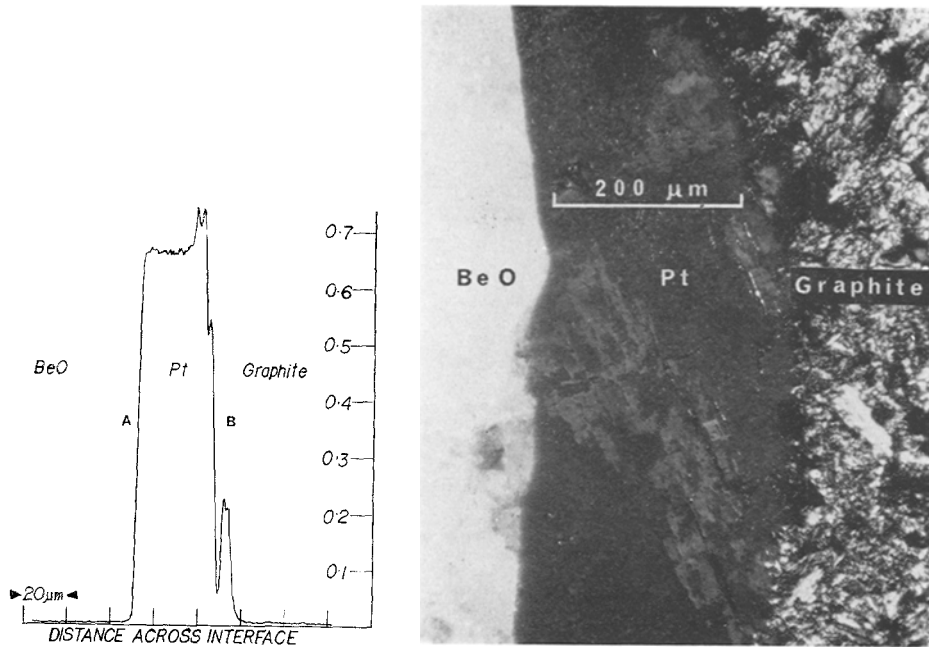


Figure 2 Electron probe trace and polarized light optical micrograph of a BeO/Pt/graphite couple (Type 1 reaction) The “sharp discontinuity” between BeO and Pt is shown at A and the movement of Pt into pores in the graphite at B. Slope of the near-vertical trace line A is due to the beam spot size. Heated in vacuum at 1500°C for 17 h.

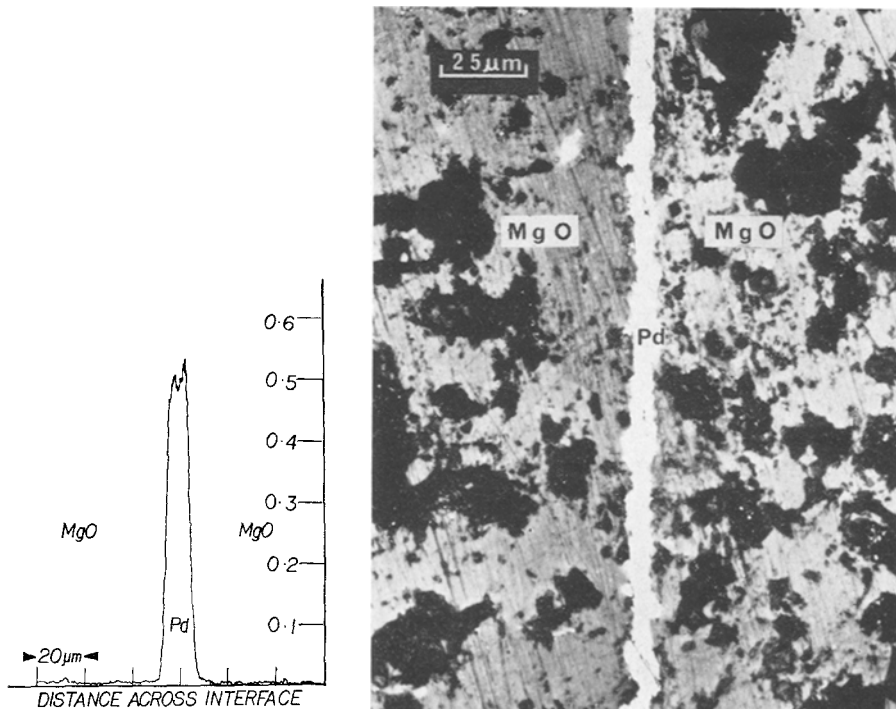


Figure 3 Electron probe trace and optical micrograph of a MgO/Pd/MgO couple (Type 1 reaction) emphasizing discontinuity between ceramic and metal. Heated at 1100°C in air for 16 h.

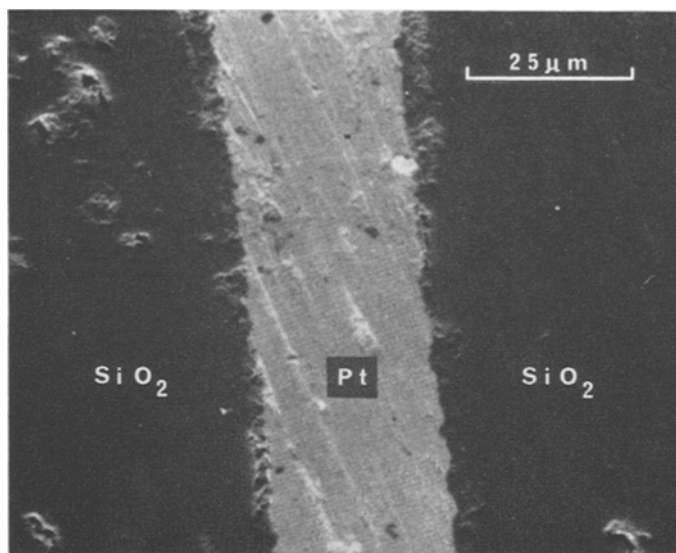


Figure 4 Emissive (filtered) scanning electron micrograph of a vitreous silica/Pt/vitreous silica couple (Type 1 reaction). Heated at 1020°C in air for 10 h.

A Cambridge Mark 2-A stereoscan instrument capable of 20 nm resolution was used for scanning electron microscopy. All sectioned and polished couples, whether Au-coated or not, were initially heated at 100°C for several days before observation to prevent outgassing from oxide pores during electron bombardment. Uncoated and Au-coated couples were photographed at voltages from 3 to 30 kV in "emissive" and "reflective" modes (i.e. filtered and unfiltered).

Polished sections were carbon-coated, and characteristic  $K\text{-}\alpha$ 's of selected elements monitored as an electron probe traversed the ceramic-metal interfaces. A JEOL model JXA3 electron probe microanalyser was used with an accelerating voltage of 15 to 25 kV and a specimen current of 0.1 A. The beam resolution was 2  $\mu\text{m}$  and the rate of traverse 10  $\mu\text{m min}^{-1}$ .

### 3. Observations and results

#### 3.1. Surface or microscopic reaction

An electron probe trace, monitored for Pt  $K\text{-}\alpha$ 's, of a BeO/Pt/graphite couple, heated in vacuum at 1500°C for 17 h without pressure is shown in Fig. 2 alongside an optical micrograph using polarized light. The oxide/metal interface is a near-perfect match, the most striking feature being the absence of metal diffusion into the ceramic. The characteristic X-rays are cut off abruptly at the interface over a distance of less than 3  $\mu\text{m}$ , which is only nominally greater than

the resolution of the microanalyser. Platinum has moved however into the pores of the graphite as indicated by the peaks near the Pt/graphite interface.

Fig. 3, a Pd  $K\text{-}\alpha$  probe trace of an MgO/Pd/MgO couple, heated at 1100°C for 16 h in air, shows that at the resolution of the instrument ( $\sim 2 \mu\text{m}$ ) Pd does not diffuse into MgO; and the converse experiment shows that Mg does not diffuse into Pd. A confirmatory experiment has also been carried out on a ZrO<sub>2</sub>/Pt/ZrO<sub>2</sub> couple.

Figs. 4 and 5 are emissive (filtered) scanning electron micrographs of vitreous silica/Pt/vitreous silica, and Al<sub>2</sub>O<sub>3</sub>/Au/Al<sub>2</sub>O<sub>3</sub> couples respectively (both at 1020°C in air for 10 h). At a resolution of 20 nm, the transition from oxide to metal is abrupt. This is in agreement with the observations made with the transmission electron microscope, where, as described in Section 4, the thickness of the bonding phase was found to be of the order of 10 nm except where surface tension effects predominated. A typical optical micrograph of this type of bond, and corresponding to the probe trace, is shown in Fig. 3.

Glass and fused silica/metal couples have been successfully tested under vacuums of  $10^{-4} \text{ Nm}^{-2}$  at normal and elevated temperatures. Fig. 6 is a Pyrex tube incorporating a Pyrex/Au/Pyrex seal which has been vacuum tight for one year. Oxide/metal bonds have not been vacuum tested

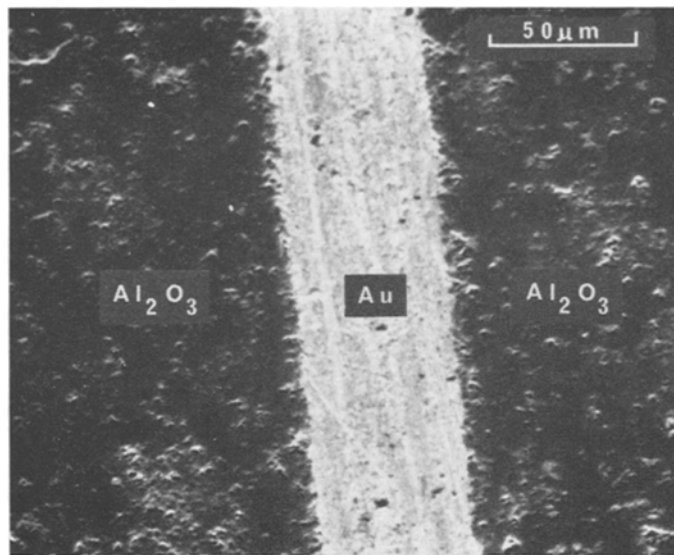


Figure 5 Emissive (filtered) scanning electron micrograph of an  $\text{Al}_2\text{O}_3/\text{Au}/\text{Al}_2\text{O}_3$  couple (Type 1 reaction). Heated at  $1020^\circ\text{C}$  in air for 10 h.

TABLE IV Shear Rupture Tests of ceramic/metal/ceramic couples (Type 1 reaction)

Couple	Temperature $^\circ\text{C}$	Time, h	Torque inch-pounds
$\text{Al}_2\text{O}_3/\text{Pt}/\text{Al}_2\text{O}_3$	835	16	negligible
$\text{Al}_2\text{O}_3/\text{Pt}/\text{Al}_2\text{O}_3$	1016	16	53
$\text{Al}_2\text{O}_3/\text{Pt}/\text{Al}_2\text{O}_3$	1055	16	108*
$\text{MgO}/\text{Pt}/\text{MgO}$	810	16	0.2
$\text{MgO}/\text{Pt}/\text{MgO}$	960	2	40*
$\text{MgO}/\text{Pt}/\text{MgO}$	1090	2	46*
$\text{Al}_2\text{O}_3/\text{Au}/\text{Al}_2\text{O}_3$	1000	4	69*
$\text{Al}_2\text{O}_3/\text{Araldite}/\text{Al}_2\text{O}_3$	—	—	108*

\*Failure in ceramic phase not at the bond. Variations in compact characteristics therefore become critically important.

as yet because of difficulties related to couple size and shape. It is, however, reasonable to expect that any oxide of near theoretical density, or at least with an isolated pore system might also be vacuum-tight.

In addition, a capacitor made by reaction welding Pt/MgO/Pt has shown good admittance stability at high frequency ( $10^9$  herz) and high temperature ( $1100^\circ\text{C}$ ).

As shown in Table IV most couples collapse by failure in the ceramic phase. The optimum conditions for the reaction depend largely on the choice of the metal and the ceramic. However, it is critical that the melting point of the lowest

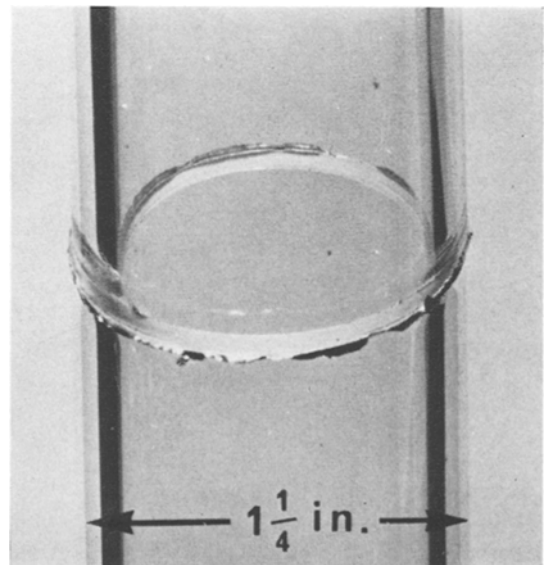


Figure 6 Pyrex/Au/Pyrex couple which has held vacuum of  $10^{-4} \text{ Nm}^{-2}$  for one year.

melting component (commonly the metal) should not be exceeded.

### 3.2. Bulk or macroscopic reaction

In contrast to the microscopic surface reaction under Section 3.1 above, diffusion plays an important role in this reaction with non-noble metals, and Table V lists the strength of some

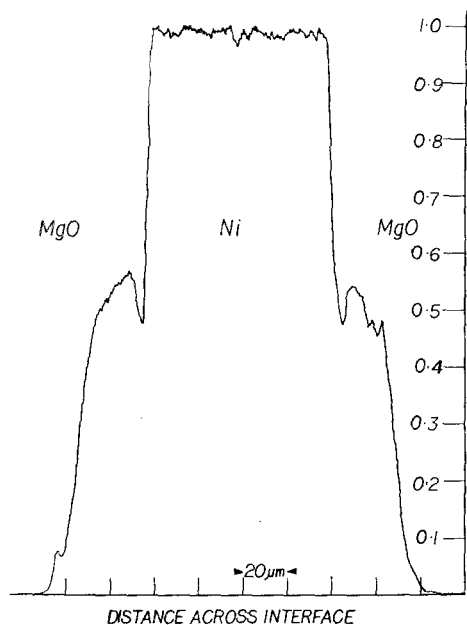


Figure 7 Electron probe trace and optical micrograph of an MgO/Ni/MgO couple (Type 2 reaction) showing penetration of Ni into the MgO.

TABLE V Shear rupture tests of ceramic/metal/ceramic couples (Type 2 reaction)

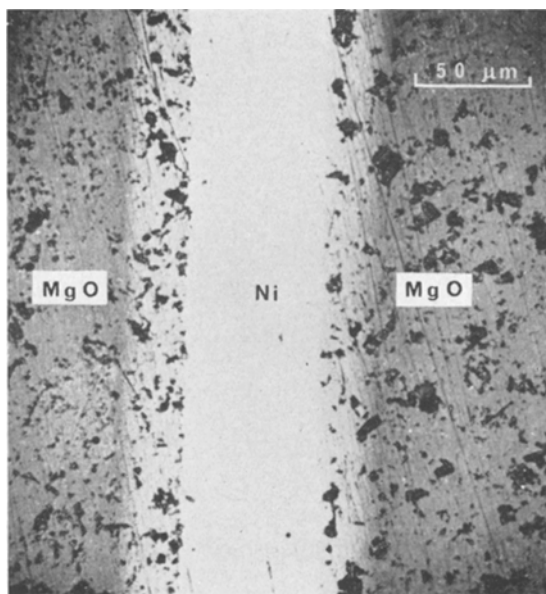
Couple	Temperature °C	Time, h	Torque inch-pounds
BeO/Ni/BeO	1100	17	85*
Al <sub>2</sub> O <sub>3</sub> /Ni/Al <sub>2</sub> O <sub>3</sub>	1050	2	29
Al <sub>2</sub> O <sub>3</sub> /Ni/Al <sub>2</sub> O <sub>3</sub>	1100	2	65
Al <sub>2</sub> O <sub>3</sub> /Ni/Al <sub>2</sub> O <sub>3</sub>	1055	16	44
Al <sub>2</sub> O <sub>3</sub> /Ni/Al <sub>2</sub> O <sub>3</sub>	1155	2	39*
Al <sub>2</sub> O <sub>3</sub> /Ni/Al <sub>2</sub> O <sub>3</sub>	1155	17	55*

\*Failure in the ceramic phase not at the bond. Variations in compact characteristics therefore become critically important.

representative bonds formed under different conditions.

Fig. 7 is typical of this type of reaction and shows an electron probe trace/optical micrograph composite of a MgO/Ni/MgO couple that had been heated in air at 1100°C for 16 h. The Ni  $K\text{-}\alpha$  signal in the probe scan reduces abruptly to 50% at the interface, corresponding to NiO which has a lattice parameter virtually identical to MgO. The signal then decreases gradually to zero over a distance of some 40  $\mu\text{m}$ . No trace of Mg could be detected in the Ni foil.

Fig. 8 shows polarized light optical (a) and reflective (unfiltered) scanning electron micrographs (b) of the same couple, confirming the extent of the substantial diffuse layer between the



metal and the original oxide. The structural continuity in such a couple is remarkable and is shown in the reflective (unfiltered) scanning electron micrographs of Fig. 9a and b. The outlined section in Fig. 9a is shown enlarged in Fig. 9b.

#### 4. Reaction mechanisms

There seems little doubt that Type 2 bonding is a bulk process involving diffusion controlled chemical reactions. Type 1 bonding however is clearly confined to reactions at or near the ceramic-metal interface, as is evident from the micrographs and electron probe traces.

Some aspects of the Type 1 reaction have also been studied by Klomp [8, 9] who suggests an evaporation mechanism of the metal onto the oxide. He proposes a criterion for bonding based on a minimum metal vapour pressure which, in turn, stipulates the temperature conditions. In contrast to the work described here, Klomp's bonding is invariably carried out in hydrogen.

Direct observation in a transmission electron microscope [14, 15] shows that, at least under vacuum conditions, vapour transport is not important and that a surface reaction proceeds with the formation of an intermediate phase.

Typically, a reaction was observed at about 1100°C between small magnesia particles (approximately 10 to 200 nm diameter) and the

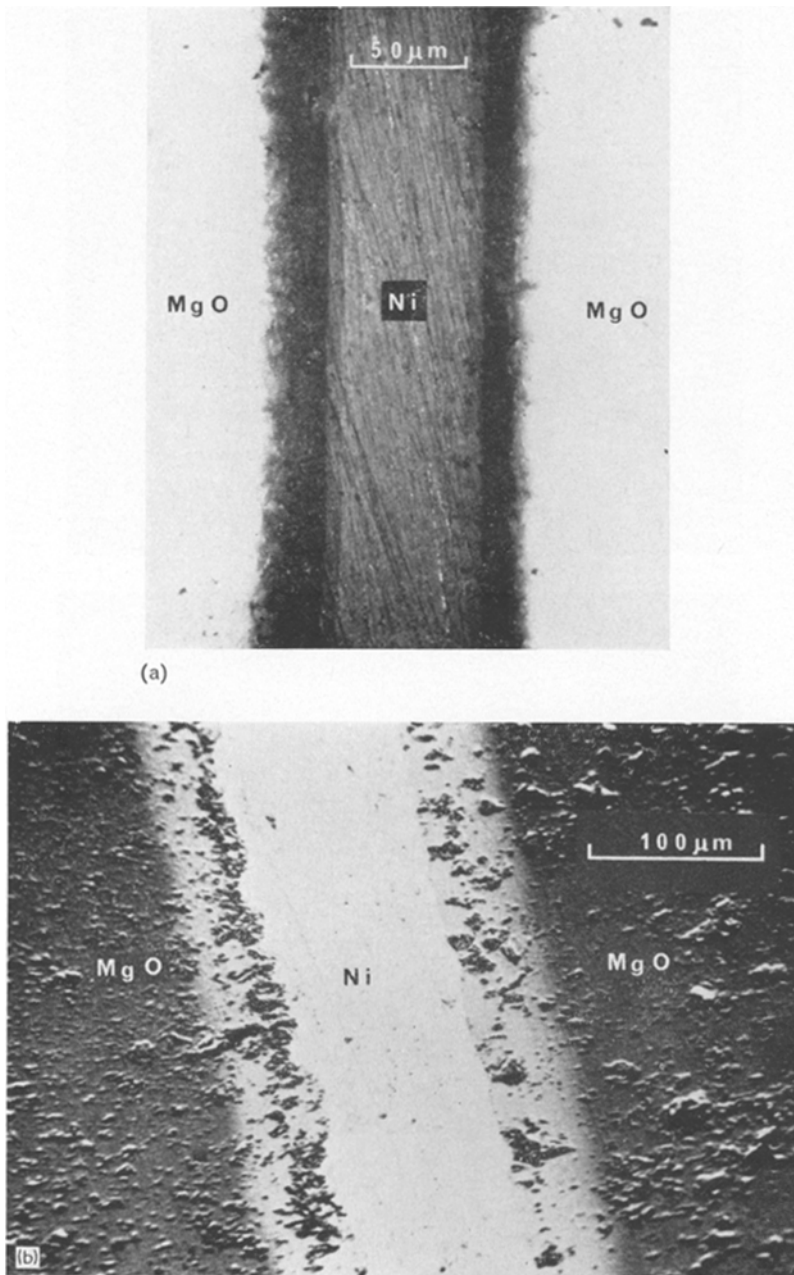


Figure 8 Polarized light optical (a) and non-coated reflective (unfiltered) scanning electron micrograph (b), emphasizing the substantial diffusion layer between Ni metal and original oxide.

palladium support grid in the hot stage of an electron microscope. At this temperature which is 450°C below the melting point of palladium, a liquid-like phase formed only where the metal and ceramic were in contact. This phase extended over (wet) the magnesia surface as fingers or en

masse. Thickness fringes, which can be seen during the reaction indicate that it is one in which the lattice planes are maintained parallel and planar at a relatively high order of perfection. This precludes the reaction being a “bulk” reaction and clearly indicates that the crystal

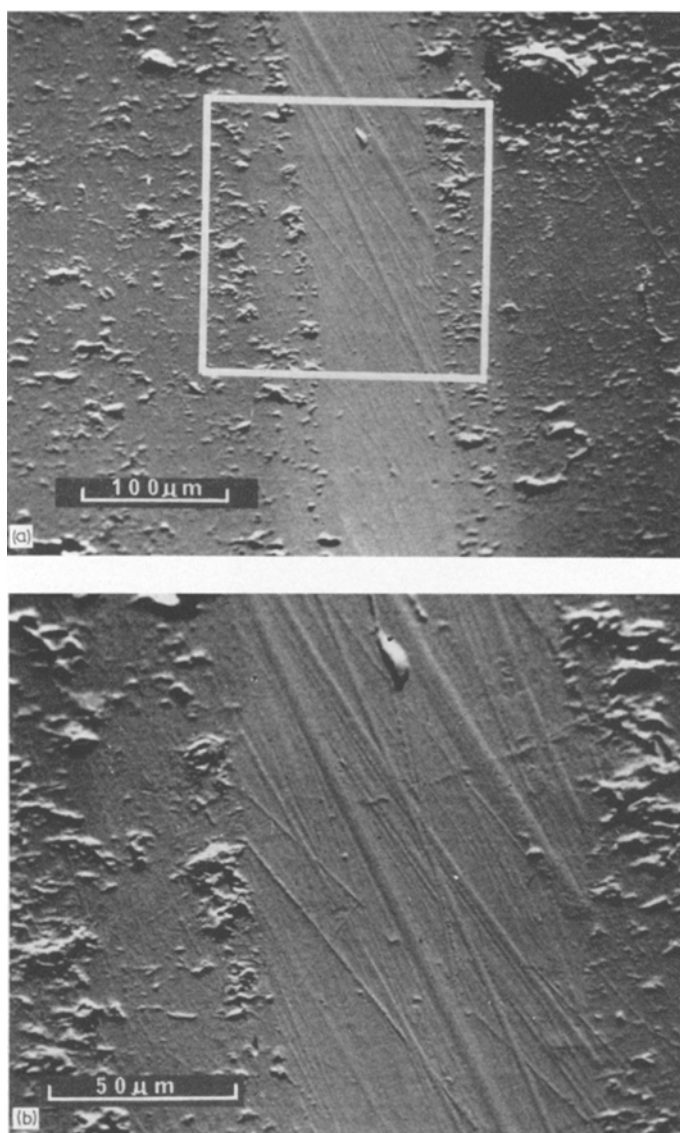


Figure 9 Au-coated, reflective (unfiltered) scanning electron micrographs showing structural continuity across the couple. Fig. 9b is an enlargement of the outlined area in Fig. 9a.

material is removed via a surface reaction involving depths of a few unit cells to several tens of nanometers. If quenched to near liquid nitrogen temperature (approximately  $-110^{\circ}\text{C}$ ) in a time of about one second (Fig. 10) the magnesia still exhibits thickness fringes. This indicates that even under quench conditions little stain is introduced into the magnesia crystals and the bond remains strong.

As the reaction proceeds a wide variation in contact angle between the liquid-like phase and

the magnesia crystals is observed, and angles as low as  $65^{\circ}$  were measured (Fig. 10). This is in marked contrast to the contact angle of  $110^{\circ}$  found between a (100) magnesia surface and small spheres of palladium after crystallization of the metal from a temperature above the melting point of palladium.

Heavy contrast observed in the liquid-like phase region, even in neck areas of 3 to 5 nm diameter, provides unequivocal evidence for a density of point defects comparable to that in a



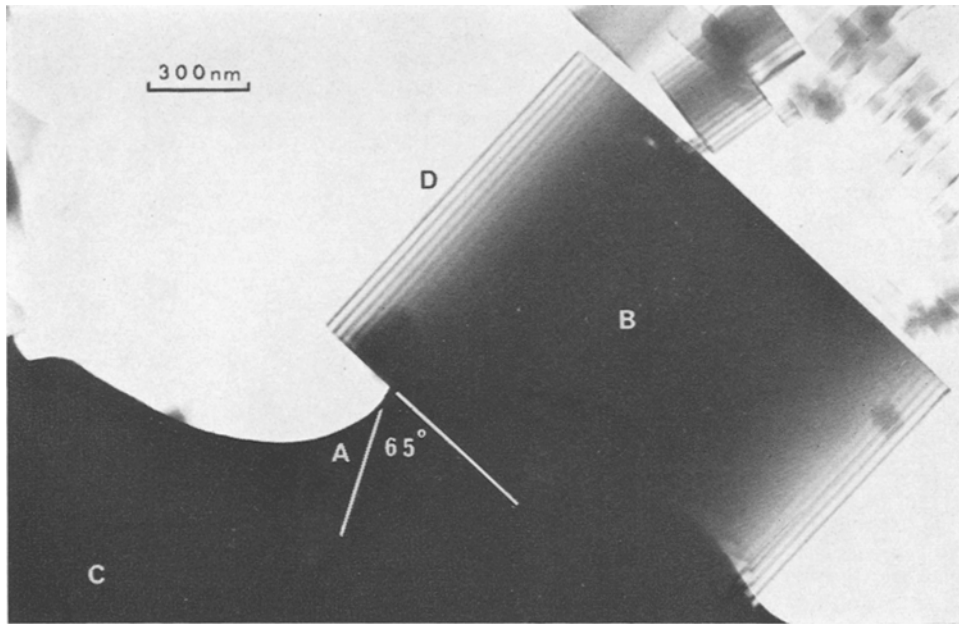


Figure 10 A quenched MgO cube, B, and Pd support grid, C, with amorphous bonding phase, A. Thickness fringes, D, indicate maintenance of crystal plane parallelism at high accuracy. Contact angle of  $65^\circ$  is shown between amorphous phase and the (100) MgO surface.

conventional liquid. This contrast is maintained on cooling (Fig. 10) showing that the bonding phase does not crystallize.

It is clear from these observations that a definite reaction takes place at the interface between oxides and noble metals.

## 5. Summary

Two types of reaction have been observed and applied to the welding of ceramics to metals and other ceramics.

Type 1, a surface reaction between oxide ceramics and noble metals which involves oxide depths of a few unit cells to several tens of nanometers and is therefore microscopic in character, maintains a "sharp discontinuity" at the interface, and is not apparently time-dependent.

Type 2, a bulk reaction between oxide ceramics and other transition metals which is time-dependent and macroscopic in character, producing a diffuse interface of compositional variations.

Both reactions have common characteristics and occur:

(a) below the melting point of the lowest melting component. In fact, in contrast to standard brazing techniques, it is imperative that the

temperature does not exceed the melting point of any component at any time.

(b) in any atmosphere compatible with all components at the operating temperature, (c) under little or no pressure (about  $100 \text{ kNm}^{-2}$ ), (d) without deformation.

No detailed mechanism is proposed for at least the Type 1 reaction since none of the standard approaches predict, at least in any obvious way, the formation of a liquid-like intermediate phase at temperatures below, and often far below, the melting point of either component. It would appear to be significant that the reaction proceeds with a variety of crystal types and with glasses; and that for a glass of lower softening point the reaction temperature is lower.

Clear evidence of a diffusion mechanism is observed in the Type 2 reaction. To this extent it is therefore more easily understood than the Type 1 reaction. In specific instances, however, details of the system may be extremely complex as the extensive literature on mixed oxide chemistry indicates. The point we wish to make here is that sufficient compatibility in structural parameters can be achieved between certain materials to lead to the formation of strong ceramic-metal bonds.

## Acknowledgements

We acknowledge the support of Dr K. D. Reeve and Mr E. Ramm of the AAEC Research Establishment for providing some of the  $\text{Al}_2\text{O}_3$  and MgO specimens, Mr P. K. Schultz at the Australian Mineral Development Laboratories for carrying out the electron probe micro-analyses, and the Department of Ophthalmology, University of Melbourne for making their scanning electron microscope available.

## References

1. For recent reviews on the art see for example A. ROTH, "Vacuum Sealing Techniques" (Pergamon Press, Oxford, 1966) p. 197 (see also Reference 2).
2. W. H. KOHL, "Handbook of Materials and Techniques for Vacuum Devices" (Reinhold Publishing Co, New York, 1967) Chapter 15.
3. F. TANK, "Method of Forming a Vacuum-tight Bond between Ceramics and Metals," U.S. Patent 2564738 (Application July 1947).
4. G. F. ERICKSON, "Ceramic to Metal Bonding Process," U.S. Patent 3214833 (Application September 1962).
5. H. J. DE BRUIN, "Method for Bonding Beryllium Oxide to Graphite," U.S. Patent 3300852 (Application February 1964).
6. A. G. BUYERS, "Ceramic-Metal Seal," U.S. Patent 3254403 (Application November 1964).
7. N. V. PHILIPS, "Procédé permettant d'assembler hermétiquement un objet métallique et des matériaux céramiques," Gloeilampenfabrieken French Patent No. 1545493 (Application November 1966).
8. J. T. KLOMP, *Sci. Ceramics*, **5** (1970) 501.
9. *Idem*, "Adhesion Bonding of Metals to Ceramics and Glasses," 72nd Annual Meeting of American Ceramic Society, Philadelphia, May (1970).
10. A. S. DARLING, G. L. SELMAN, and R. RUSHFORTH, *Platinum Metals Rev.* **14** (1970) 54.
11. *Idem*, *ibid*, **14** (1970) 95.
12. C. A. CALOW, P. D. BAYER, and I. T. PORTER, *J. Mater. Sci.* **6** (1971) 150.
13. C. A. CALOW and I. T. PORTER, *ibid*, **6** (1971) 156.
14. A. F. MOODIE and C. E. WARBLE, paper presented at XXII International Congress of Pure and Applied Chemistry, Sydney, Australia, August (1969).
15. *Idem*, to be published, *Phil. Mag.*
16. H. J. DE BRUIN, A. F. MOODIE, and C. E. WARBLE, Proceedings of the Fourth Australian Ceramic Conference, Monash University, Melbourne, Australia, August (1970).
17. *Idem*, paper presented at Materials for the Electrical and Electronics Industries Conference, Perth, Australia, August (1971).
18. *Idem*, *J. Aust. Ceram. Soc.*, **7** (1971) 57.
19. CSIRO and the Flinders University of South Australia, "Chemical Bonding of Metals to Ceramic Materials," Australian Patent Application, PA 25585/71.

Received 11 November 1971 and accepted 3 February 1972.